LAWRENCE
LIVERMORE
NATIONAL
LABORATORY

LLNL-TR-760731

Deformation Mechanisms in Body-Centered Cubic Metals at High Pressures and Strain Rates

L. Hsiung

October 30, 2018

Disclaimer

This document was prepared as an account of work sponsored by an agency of the United States government. Neither the United States government nor Lawrence Livermore National Security, LLC, nor any of their employees makes any warranty, expressed or implied, or assumes any legal liability or responsibility for the accuracy, completeness, or usefulness of any information, apparatus, product, or process disclosed, or represents that its use would not infringe privately owned rights. Reference herein to any specific commercial product, process, or service by trade name, trademark, manufacturer, or otherwise does not necessarily constitute or imply its endorsement, recommendation, or favoring by the United States government or Lawrence Livermore National Security, LLC. The views and opinions of authors expressed herein do not necessarily state or reflect those of the United States government or Lawrence Livermore National Security, LLC, and shall not be used for advertising or product endorsement purposes.

This work performed under the auspices of the U.S. Department of Energy by Lawrence Livermore National Laboratory under Contract DE-AC52-07NA27344.

Deformation Mechanisms in Body-Centered Cubic Metals at High Pressures and Strain Rates

Luke L. Hsiung (16ERD043)

Abstract

Deformation mechanisms of single-crystal Ta oriented at four different crystal orientations: [001], [011], [$\bar{1}$11], and [$\bar{1}$23] and shock-compressed at two different peak pressures: 50 GPa and 65 GPa using a gas gun flyer-plate impact method have been studied. The main objective of this investigation is to elucidate the shock-induced shear transformations: deformation twinning and the α (bcc) → ω (pseudo-hexagonal) transition which were observed to take place in shock-deformed polycrystalline Ta at 30 GPa when the formation of low-energy cellular dislocation structure and polygonization due to dynamic recovery becomes suppressed. Emphasis is placed on the effects of crystal orientation and strain rate on the shock-induced dynamic recovery and shear transformations. Novel mechanisms for the formation of cellular dislocation structure and polygonization based on the coupling reactions of the ½<$\bar{1}$11> coplanar dislocations in the {$\bar{1}$01} slip planes are proposed to elucidate the competition between dynamic recovery and shear transformations.

Background and Research objectives

Preceding studies of dynamic behavior of polycrystalline Ta and Ta-W alloys shock-deformed at 30 and 45 GPa have revealed the onset of shock-induced deformation twinning and α (body-centered cubic) → ω (pseudo-hexagonal) transition [1,2]. The pseudo-hexagonal ω phase contains 3-atoms/unit cell with the lattice constants: $a_\omega = \sqrt{2}\ a_\alpha = 0.468$ nm and $c_\omega = (\sqrt{3}/2)\ a_\alpha = 0.286$ nm ($c_\omega/a_\omega = 0.611$), where a_α is the lattice parameter of α (bcc)-lattice. The formation of shock-induced α → ω transition is fascinating since Ta exhibits no pressure-induced phase transformation under hydrostatic pressures up to 174 GPa according to the studies reported in the open literature [3,4]. For pressure-induced phase transformation under hydrostatic-pressure (or isentropic) conditions, Ta may undergo the α → ω transition as the Gibbs free energy of a competing phase ω becomes less than that of the parent phase α above a critical pressure (P_{eq}). That is, the pressure-induced α → ω transition occurs when the pressure increases above P_{eq}. However, it is also known that material shock-compressed under the Hugoniot-adiabatic conditions can lead to a considerable increase in temperature, and the higher the applied pressure the higher the overheat temperature [5]. This means a higher pressure is required to achieve an equivalent volume (or density) in the Hugoniot-adiabatic conditions than in the isentropic conditions. Accordingly, the P_{eq} for the pressure-induced α → ω transition, if it does exist, should be higher than 174 GPa under the Hugoniot conditions. However, the occurrence of the α → ω transition in shock-compressed Ta and Ta-W alloys at much lower pressures: 30 and 50 GPa reveals that the Hugoniot equation of state (EOS) is insufficient to explain the α → ω transition occurred in shock-compressed tantalum. However, an implication may be drawn from the results of dislocation substructure formed in polycrystalline Ta shocked at 30 GPa ($\dot{\epsilon} \sim 10^4\ s^{-1}$) using an HE-driven spherical cap method [2] as shown in Figure. 1. Here, neither twin nor ω phase but a cellular dislocation structure was observed in the [001]-oriented grain shown in Figure 1a. On the other hand, ω plates in association with a quasi-uniformly distributed high-density dislocation structure was observed in the [011]-oriented grain shown in Figure 1b. These results imply that different strengthening mechanisms, associated with different increments of stored strain energy, take place in grains with different crystal orientations under high pressure and strain-rate conditions. The grain orientation can play an important role in the shock-induced α → ω transition, which apparently takes place when the formation of low-energy cellular dislocation structure is suppressed. It is postulated that the increase in internal energy due to the stored strain energy raising from different dislocation arrangements should also be considered for the change in free energy under dynamic conditions. A deformation of a crystalline material can always be described as the sum of a change in volume and a change in shape at constant volume (i.e., shear). Assuming a given structure, the change in volume can be recovered when the load is removed.

The change in shape, on the other hand, may or may not be recovered. The part of shear that is recoverable is elastic, and the part that remains is plastic. Thus, plastic deformation through shear by dislocation glide plays a vital role in shock-induced deformation twinning and α → ω transition. Line density and arrangement of high-density stored dislocations (which can alter the free energy significantly by changing the internal energy) shall also be considered as a crucial factor to elucidate the onset of shock-induced deformation twinning and α → ω transition, i.e., shear transformations, in tantalum. A novel dislocation-based mechanism has been proposed and reported elsewhere [6] to rationalize the transition of dislocation glide to shear transformations in shock-deformed tantalum: shear transformations. Twinning and the α → ω transition take place as an alternative deformation mechanism to accommodate the high-strain-rate straining when the shear stress required for dislocation multiplication exceeds the threshold shear stresses for twinning and the α → ω transition.

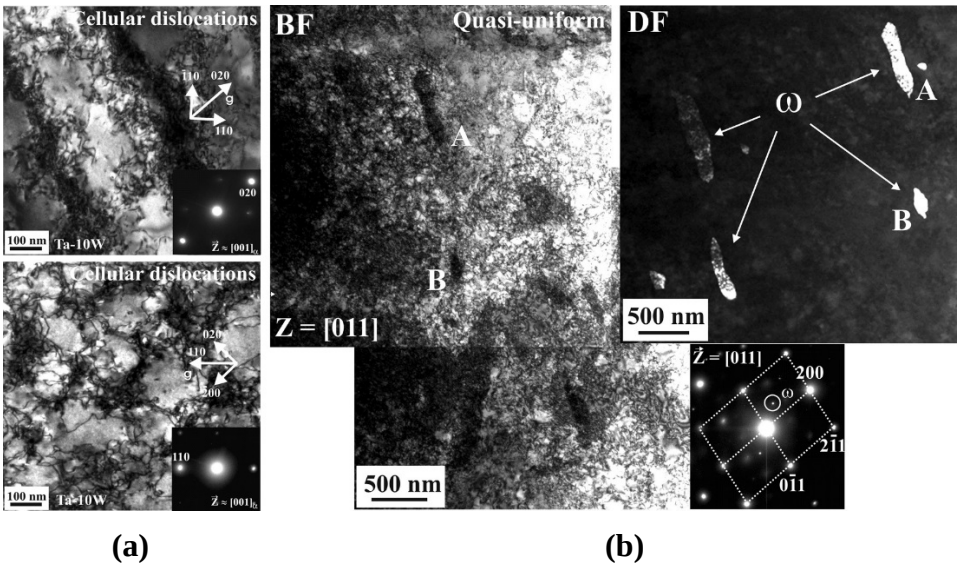

Figure 1. Bright-field (BF) and dark-field (DF) TEM images showing the formation of (a) cellular dislocation structure (the early stages of polygonization) in the [001]-oriented grain and (b) ω plates associated with quasi-uniformly distributed dislocation structure in the [011]-oriented grain of the same Ta sample shocked at 30 GPa ($\dot{\epsilon}$ ~10^4 s^{-1})

There are two distinctly different dislocation arrangements in addition to the line density (ρ) can affect the internal energy of shocked-deformed tantalum. The first type of dislocation arrangement is a quasi-uniform random arrangement, which has a local line density: $\rho = {}^{1}/_{l^2}$, where l is the average (local) line spacing. The second type of dislocation arrangement is a heterogeneous arrangement of dislocation cells, which composes of cell wall with high dislocation density (ρ_w) and cell interior with low dislocation density that was often observed in large-stain deformed metals and alloys. It is of worth noting that dislocations develop into cell structures are caused by dynamic recovery which involve cross-slip of screw dislocations [7]. The dynamic-recovery reactions in plastic deformation of metals and alloys involve mainly the following dislocation interactions: (i) the interactions of dislocations with different Burgers vectors ($\boldsymbol{b_1}$ and $\boldsymbol{b_2}$) to form a "node" or "junction" dislocation with a Burgers vector ($\mathbf{b_3}$), i.e., $\boldsymbol{b_1} + \boldsymbol{b_2} \rightarrow \boldsymbol{b_3}$ when $\boldsymbol{b_3^2} < \boldsymbol{b_1^2} + \boldsymbol{b_2^2}$, (ii) the mutual annihilation of screw and edge dislocations with opposite Burgers vectors ($\pm\boldsymbol{b}$) in the same slip plane**,** and (iii) the interactions of dislocations to cluster into low-energy structure and polygonization, i.e., cellular dislocation structure and tilt walls, in which the strain energy per unit length of participant dislocations is minimized [8]. Among those dislocation interactions, the dislocation clustering into cells and tilt walls are especially noticeable during a transient process of

shock-deformation that usually lasts only a few micro-seconds. It is known that the mechanical energy is transformed into heat during plastic straining and only a small portion of the energy input is stored in the material in the form of dislocations. During high strain-rate straining, many dislocations are trapped mutually before they can reach grain boundaries and free surfaces, and it is expected that dislocation interactions would follow the general principles of minimization of free energy to generate mechanically stable equilibrium configurations. The glide dislocations configurations tend to approach the minimum energy per unit length of dislocation line when the dislocation density and thus interactions among dislocations increase. It is the task of deformation and work-hardening theory to unravel the interconnections between the generation rate of mobile dislocations, the propagation distance of mobile dislocations, and the interactions and arrangement of dislocations. The alteration of dislocation configurations which lead to the internal-energy minimization through the reduction of the total stored strain-energy, i.e., the sum of the energy stored in the dislocation self-energy and the longer-range interaction energy, are intimately related to the competition between the dynamic recovery and the shock-induced shear transformations (deformation twinning and the $\alpha \rightarrow \omega$ transition). The goals of current study aim to (i) to unravel the underlying mechanisms for the development of low-energy cellular structure and polygonization, (ii) clarify the governing factors for the suppression of dynamic recovery. Emphasis is placed on the effect of crystal orientation and strain-rate on the competition between dynamic recovery and shear transformations.

Scientific Approach and Accomplishments

Gas gun flyer-plate impact experiments and post-shock analysis and characterization

Ta single-crystal rods (99.99% pure) with dimensions of ~5 cm long and ~1.2 cm in diameter were recieved from Goodfellow Cambridge Ltd, London, UK. The interstitial impurities (ppm in weight) are (O: 25; N: <10; H: <5; C: <10). A total of eight disc-shaped specimens with dimensions of ~3 mm thick and ~7.6 mm in diameter were sliced and prepared from Ta single-crystal rods with the surface normal of specimens paralellel to the following four different orientations: [001], [011], $[\bar{1}11]$, and $[\bar{1}23]$. Both the top and bottom surfaces of each sample disc were ground and polished with colloidal diamond to ensure that the two surfaces are parallel to each other, within an error less than 3 microns. Before being employed for gas-gun recovery experiments, the single-crystal specimens were painted with different colors for the four specified orientations. Gas gun flyer-plate impact experiments were performed at CalTech using a 40 mm bore single-stage powder gun. Four single-crystal Ta specimens were encapsulated in a target assembly that was made of stainless-steel capsule and plug. Two shock-compression experiments were performed at velocities of 0.355 km/s and 0.476 km/s, respectively. The peak shock pressures of ~50 GPa and ~65 GPa for the two experiments were determined from the impactor velocity and standard impedance matching. The capsules were recovered intact from both experiments. The post-shocked Ta single-crystal specimens were then removed from the recovered capsules and were subsequently analyzed using a Philips PW-3720 x-ray diffractometer and the results are shown in Figure 2a. Here, extra diffraction peaks (marked by arrows) presumably caused by either shear transformations or polygonization, can be clearly seen from the single-crystal specimens shock-deformed at 50 GPa and 65 GPa with the mean strain rate ($\dot{\epsilon}$) approximately on the order of 10^5 s^{-1}. Effects of strain-rate and crytal orientation on shock-induced deformation substructures, particularly shear transformations (i.e., twinning and the $\alpha \rightarrow \omega$ transition) in shock-recovered specimens were further examined using a Phillips CM300 field-emission transmission electron microscope (accelerating voltage of 300 kV). TEM results are shown in Figures 2a for specimens shocked at 50 GPa and Figure 2b for specimens shocked at 65 GPa. Clearly, shock-induced shear transformations (i.e., deformation twinning and the $\alpha \rightarrow \omega$ transition) occurred in all four single-crystal specimens shocked at 50 GPa. However, for the case of 65 GPa, shock-induced polygonization (i.e., the formation of tilt walls) occurred in the [001]- and the $[\bar{1}11]$-oriented specimens and shock-induced shear transformations occurred in the [011]- and $[\bar{1}23]$-oriented specimens. It is worth noting that the volume fraction of twin- and ω-plates as high as 50% were found to form in the [011]-oriented specimens shocked at 50 GPa and 65 GPa.

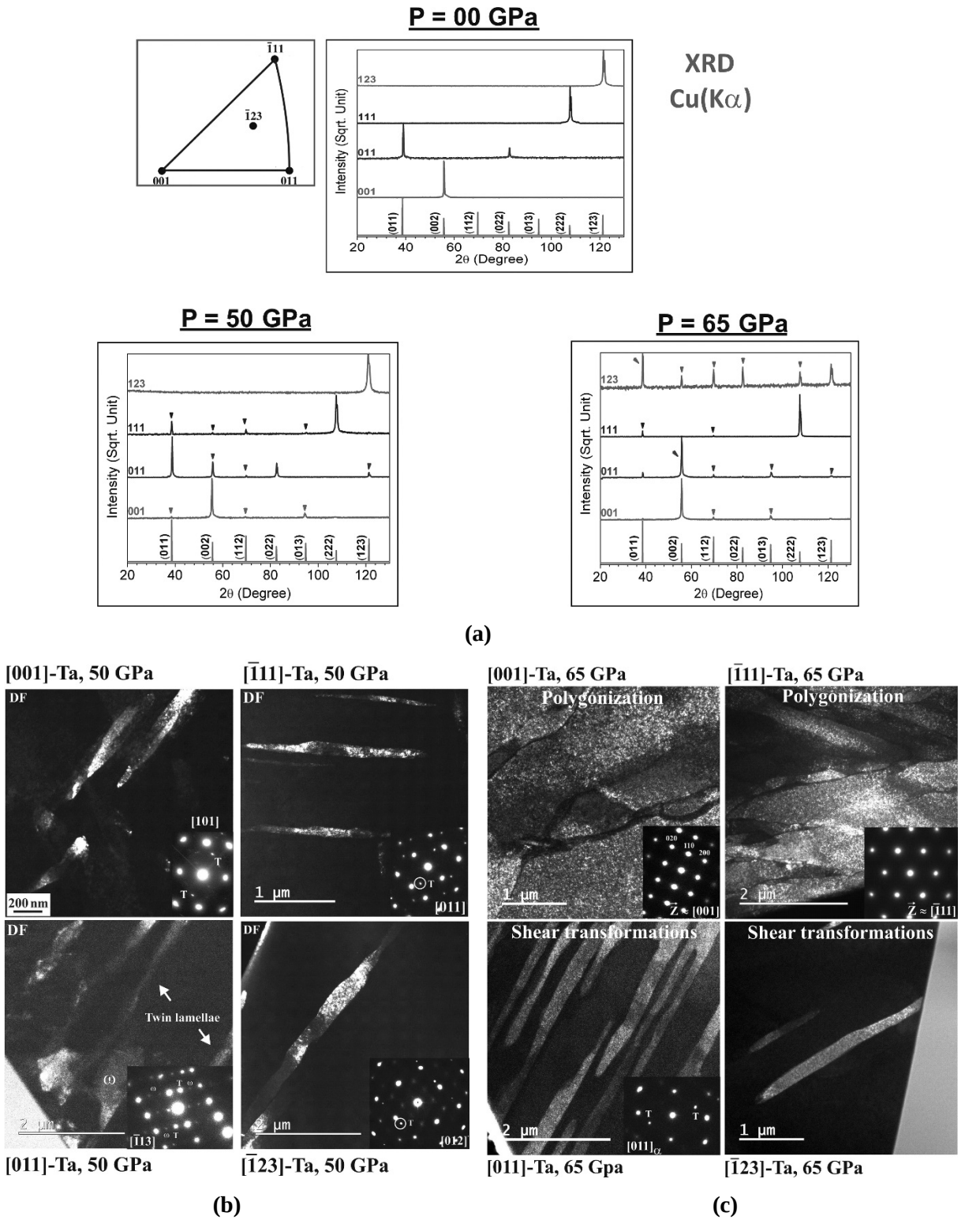

Figure 2. X-ray (a) and TEM results (b, c) obtained from shock-recovered single-crystal Ta specimens showing shock-induced shear transformations occurred in all four single-crystal specimens shock-deformed at 50 GPa. However, for the case of 65 GPa, shock-induced polygonization occurred in the [001]- and the [$\bar{1}$11]-oriented specimens and shock-induced shear transformations occurred in the [011]- and [$\bar{1}$23]-oriented specimens.

Proposed mechanisms for the formation of cellular dislocation structure and tilt walls

Results of TEM dislocation analyses obtained from the [001]-oriented grains within polycrystalline tantalum shock-deformed at 30 GPa [2] revealed that rudimentary cell-walls (see Figure 3a) formed at early stages of polygonization; tilt-walls (see Figure 3b) formed at later stages of polygonization. Both rudimentary cell-walls and tilt-walls tend to alighn parallel to the projected <101> directions (labeled as red lines) which have an angle of 35.16° with respect to the adjacent <111> Burgers vector (labeled as blue lines). Based on the dislocation-contrast and the Peach-Koehler force [9] analyses, novel mechanisms stemmed from coupling reactions of the ½<111> coplanar dislocations in the $\{\bar{1}01\}$ slip planes are proposed to unravel the formation of low-energy cellular dislocation structure and polygonization. The mechanisms involve (i) the coupling reactions of two coplanar ½[111] (**b_1**) and ½$[\bar{1}1\bar{1}]$ (**b_2**) screw dislocations in the $(\bar{1}01)$ slip planes by altering their line direction (i.e., b_1 turns clockwise and b_2 turns counterclockwise) to form an attractive pair of mixed dislocations with the line direction parallel to the ±[101] direction, (ii) the clustering of several attractive pairs into mutual stress-screening dislocation arrays to form a cell wall, and (iii) the evolution of dislocation arrays in a cell wall into a tilt wall which contains a planar array of edge-dislocations with the Burgers vector [010] (**b_3**) normal to the planar array. The proposed mechanisms are illustrated and depicted in Figure 4. The implications of the proposed mechanisms are three-fold: (i) the coupling reactions for the formation of low-energy cellular dislocation structure and polygonization is a thermally activated process and therefore can be strain-rate dependent, (ii) the coupling reactions are orientation dependent since the reactions require active coplanar slip systems in the {101} planes, (iii) the coupling reactions in the $\{\bar{1}01\}$ slip planes to form cellular dislocation structure and polygonization are prohibited in the specimens oriented at the [011] and the $[\bar{1}23]$ orientations due to lack of active coplanar slip systems. The proposed mechanisms are very well applied to rationalize the results of this study summarized in Table 1: (i) the coupling reactions in the $\{\bar{1}01\}$ slip planes to form cellular dislocation structure and polygonization become suppressed in the specimens oriented at the [011] and the $[\bar{1}23]$ orientations due to lack of active coplanar slip systems, (ii) polygonization in the [001]- and the $[\bar{1}11]$-oriented specimens shocked at 65 GPa can be attributed to adiabatic-heating enhanced dynamic recovery under Hugoniot adiabatic conditions. Yet, the adiabatic heating has little effect on the [011]- and $[\bar{1}23]$-oriented specimens due to lack of active coplanar slip systems, and (iii) shock-induced shear transformations are prevailed in the [011]-oriented specimens shocked at 50 GPa and 65 GPa due to the suppression of coupling reactions**,** (iv) the volume fraction of shock-induced twin- and ω-plates formed in the [011]-Ta specimens is > 50vol.%, which is much higher than that formed in specimens of other orientations studied.

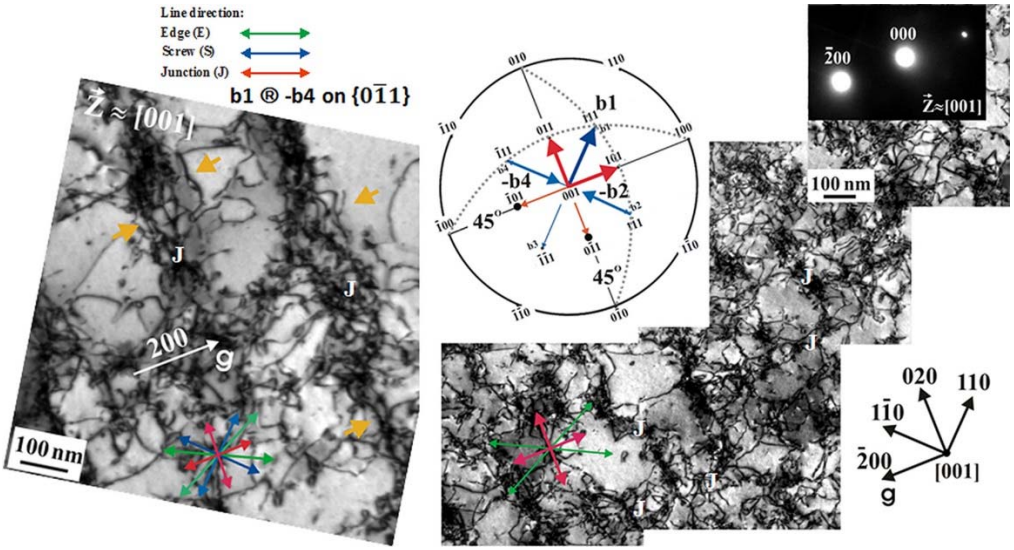

(a)

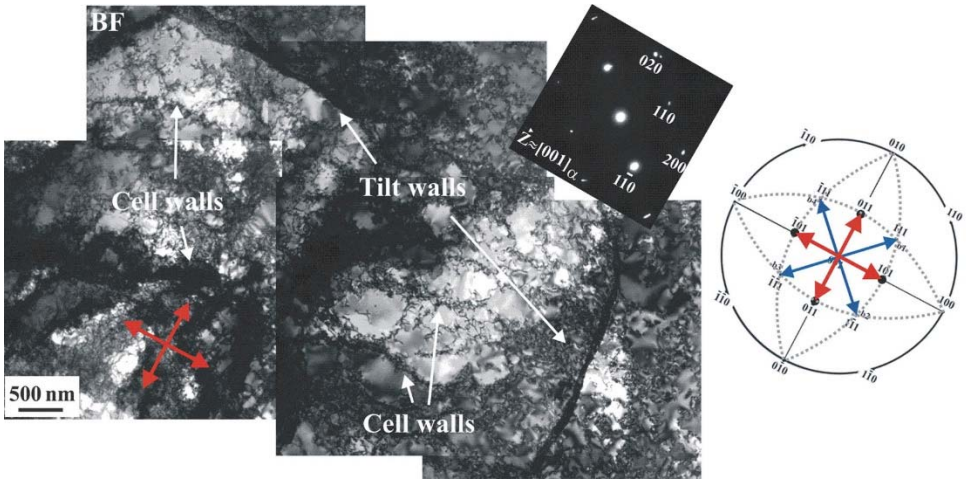

(b)

Figure 3. Bright-field TEM images displayed together with the [001] stereographic projection to show (a) the formation of rudimentary cell-walls (labeled as J) that are preferably aligned to crystallographic orientations labeled as red lines; (b) co-existence of rudimentary cell walls (formed at early stages of polygonation) and tilt walls (formed at later stages of polygonization).

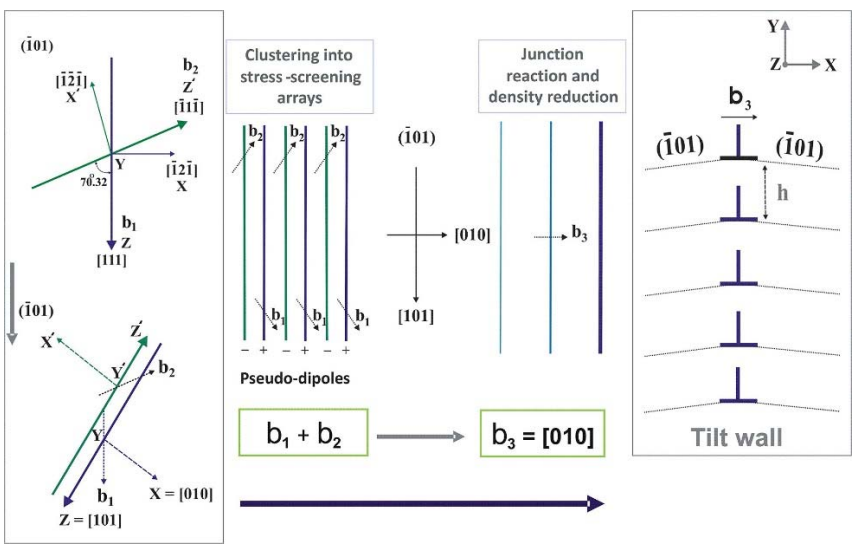

Figure 4. Schematic illustrations showing (i) the coupling reactions of two coplanar ½[111] (**b₁**) and ½[$\bar{1}1\bar{1}$] (**b₂**) screw dislocations in the ($\bar{1}$01) slip planes by altering their line direction (i.e., the line direction of **b₁** turns 35.16° clockwise and the line direction of **b₂** turns 35.16° counterclockwise) to form an attractive-pair of mixed dislocations with the line direction parallel to the ±[101] direction, (ii) the clustering of several attractive pairs into mutual stress-screening dislocation arrays for a cell wall, and (iii) the evolution of dislocation arrays through a junction reaction [½[111] (**b₁**) + ½[$\bar{1}1\bar{1}$] (**b₂**) → [010] (**b₃**)] into a tilt wall which contains a planar array of edge-dislocations with the Burgers vector [010] (**b₃**) normal to the planar array. Since it represents a wedge of additional atomic planes normal to the Burgers vector, the ($\bar{1}$01) slip plane is kinked or tilted at the wall. Note that **X** || [010], **Y** || [$\bar{1}$01], and **Z** || [101]. Both cell walls and tilt walls are aligned parallel to the <101> directions.

Impact on mission

The capability to determine deformation mechanisms will have a significant impact in the development of predictive constitutive materials models for WCI applications. With the increasing power of

supercomputers and the development of multiscale modeling techniques, it is becoming possible to develop constitutive models (e.g., strength and martensitic transformation models) parameterized entirely from first principles. These models must be validated by experimental data, but often the data are from difficult, integrated dynamic experiments, and it is hard to determine whether any disagreement attributed to erroneous parameters or missing physics. The models are typically formulated based on a working hypothesis, the dominant mechanisms, guided by years of experience but at low rates and low pressures. Experiments that directly determine mechanisms can have tremendous impact. For example, a model that assumes slip-based plasticity might be shown to need to be extended to account for the effect of twinning or phase transformation on the plastic flow rate and microstructural changes. Once demonstrated for bcc metals, the approach can be applied to material of interest to program, for example U6Nb. Since there is a strong programmatic need for constitutive model development at LLNL, and it is this need that we propose to address, developing a new capability for NNSA-related programs at LLNL.

Conclusion

Shock-induced polygonization and shear transformations [deformation twinning and the α (bcc) $\rightarrow$ ω (pseudo-hexagonal) transition] have been verified to occur in single-crystal tantalum specimens oriented at four different crystal orientations: [001], [011], [$\bar{1}$11], and [$\bar{1}$23] and shocked at two different peak pressures: 50 GPa and 65 GPa. Shock-induced polygonization mainly took place in the [001]- and [111]-oriented specimens in which the coplanar coupling reactions for dynamic recovery were prevalent. The suppression of dynamic recovery at high strain-rate did occur in the [001]- and [111]-oriented specimens shocked at 50 GPa, however, the thermally activated polygonization became prevalent when the shock-pressure further increased to 65 GPa because of adiabatic heating. Shock-induced shear transformations were prevailed in the [011]- and the [$\bar{1}$23]-oriented specimens shocked at both pressures in which the coupling reactions for dynamic recovery became suppressed due to lack of active coplanar slip systems. Novel mechanisms stemmed from the coupling reactions of the ½<111> coplanar dislocations in the {$\bar{1}$01} slip planes are proposed to elucidate the effects of crystal orientation and strain rate on the competition between dynamic recovery and shear transformations. This work was performed under the auspices of the U.S. Department of Energy by LLNL under Contract DE-AC52-07NA27344.

References

[1] Hsiung L. and Lassila D.H. 2000. "Shock-Induced Deformation Twinning and Omega Transformation in Tantalum and Tantalum-Tungsten Alloys." Acta Mater. 48, 4851-4865. https://doi.org/10.1016/S1359-6454(00)00287-1.

[2] Hsiung L. 2010. "Shock-Induced Phase Transformation in Tantalum." J. Phys.: Condens. Matter 22, 385702 (6pp). https://doi.org/10.1088/0953-8984/22/38/385702.

[3] D.A. Young, Phase Diagrams of the Elements, University of California Press, Berkeley: California (1991).

[4] Cynn H., Yoo C.S. 1999. "Equation of state of tantalum to 174 GPa," Phys. Rev. B 59, no. 13 (April): 8526-8529. https://doi.org/10.1103/PhysRevB.59.8526.

[5] Isbell W. M. 2005. Shock Waves: Measuring the Dynamic Response of Materials. London: Imperial College Press.

[6] Hsiung, L. and Campbell, G.H. 2017. "Transition of Dislocation Glide to Shear Transformation in Shocked Tantalum." MRS Advances 2, Issue 27 (Feb.): 1417-1428. https://doi.org/10.1557/adv.2017.236.

[7] Marcinkowski, M.J. 1984. "The Mechanism of Cell Wall Formation." Phys. Stat. Sol. (a) 88, 59-68. https://doi.org/10.1002/pssa.22/0830105.

[8] Hansen N. and Kuhlmann-Wilsdorf D. 1986. "Low Energy Dislocation Structure due to Unidirectional Deformation at Low Temperatures." Mater. Sci. Eng. 81, 141-161. https://doi.org/10.1016/0025-5416 (86) 09258-2.

[9] Peach M. and Koehler J.S. 1950. "The Forces Exerted on Dislocations and the Stress Field Produced by Them." Physical Review 80, no. 3 (November): 436-439. https://doi.org/10.1103/PhyRev.80.436.

Publications and Presentations

1. Hsiung, L. and Campbell, G.H. 2017. "Transition of Dislocation Glide to Shear Transformation in Shocked Tantalum." MRS Advances 2, Issue 27 (Feb.): 1417-1428. https://doi.org/10.1557/adv.2017.236.
2. "Transitions of Dislocation Glide to Twinning and Shear Transformation in Tantalum under Shock Straining." Invited presentation at 2016 MRS Fall Meeting & Exhibit, Boston, Massachusetts. November 27 – December 2, 2016.
3. "Shock-Induced Deformation Twinning and Omega Transformation in Tantalum." Invited keynote lecture at Plasticity 2018, San Juan, Puerto Rico. January 3 – 9, 2018
4. "Shock-Induced Shear Transformations: Correlation with Dislocation Arrangements." Invited presentation at 18th International Conference on the Strength of Materials: John P. Hirth Honorary Symposium, The Ohio State University, Columbus, Ohio. July 15–19, 2018

Table 1.

Schmid factors for the $\{\bar{1}01\}$ <111> slip systems, active coplanar slip systems for the coupling reactions, and the observed deformation mechanisms

Slip Plane (hkl)	Slip Direction [hkl]	Crystal Orientation ‖ Stress Axis			
		[001]	$[\bar{1}11]$	[011]**	$[\bar{1}23]$**
		Schmid Factor*	Schmid Factor*	Schmid Factor*	Schmid Factor*
$(\bar{1}01)$	[111]	0.41	0.27	0.41	0.47
	$[\bar{1}1\bar{1}]$	0.41	0.27	0	0
(101)	$[\bar{1}\bar{1}1]$	0.41	0	0	0.12
	$[1\bar{1}\bar{1}]$	0.41	0	0.41	0.35
$(0\bar{1}1)$	$[1\bar{1}1]$	0.41	0	0	0
	$[1\bar{1}\bar{1}]$	0.41	0	0	0.18
(011)	$[\bar{1}11]$	0.41	0.27	0	0
	$[\bar{1}1\bar{1}]$	0.41	0.27	0	0
$(\bar{1}10)$	[111]	0	0.27	0.41	0.35
	$[\bar{1}\bar{1}1]$	0	0.27	0	0.18
(110)	$[1\bar{1}1]$	0	0	0	0
	$[\bar{1}11]$	0	0	0.41	0
Pairs of active coplanar Slip Systems for the coupling reactions		4	3	0	< 2
Deformation Mechanisms based on TEM Observations	Polycrystal 30 GPa ($\dot{\epsilon}$ ~10^4 s^{-1})	Polygonization	Polygonization	Shear Transformations	No Data
	Single-crystal 50 GPa ($\dot{\epsilon}$ ~10^5 s^{-1})	Shear Transformations	Shear Transformations	Shear Transformations	Shear Transformations
	Single-crystal 65 GPa ($\dot{\epsilon}$ ~10^5 s^{-1})	Polygonization***	Polygonization***	Shear Transformations	Shear Transformations

*Schmid factor is a measure of resolved shear stress acting on a specific $\{\bar{1}01\}$ <111> slip system.
The coupling reactions in the $\{\bar{1}01\}$ slip planes to form cellular dislocation structure and polygonization become suppressed in the specimens oriented at the [011] and the $[\bar{1}23]$ orientations due to lack of active coplanar slip systems.*Polygonization in the [001]- and the $[\bar{1}11]$-oriented specimens shocked at 65 GPa can be attributed to adiabatic-heating enhanced dynamic recovery under Hugoniot adiabatic conditions.